Biophysical Chemistry 146 (2010) 13–24

Contents lists available at ScienceDirect

Biophysical Chemistry

journal homepage: http://www.elsevier.com/locate/biophyschem

Analysis of light-induced transmembrane ion gradients and membrane potential in Photosystem I proteoliposomes

Cristian Pablo Pennisi [a,*], Elias Greenbaum [b], Ken Yoshida [a,c]

[a] Center for Sensory–Motor Interaction (SMI), Department of Health Science and Technology, Aalborg University, Denmark
[b] Chemical Sciences Division, Oak Ridge National Laboratory, Oak Ridge, Tennessee 37831, USA
[c] Biomedical Engineering Department, Indiana University-Purdue University Indianapolis, Indiana, USA

ARTICLE INFO

Article history:
Received 25 June 2009
Received in revised form 25 September 2009
Accepted 27 September 2009
Available online 6 October 2009

Keywords:
Photosystem I
Reconstitution
Cyclic electron transport
Light-induced proton transport
Electrodiffusion model
Computer simulation

ABSTRACT

Photosystem I (PSI) complexes can support a light-driven electrochemical gradient for protons, which is the driving force for energy-conserving reactions across biological membranes. In this work, a computational model that enables a quantitative description of the light-induced proton gradients across the membrane of PSI proteoliposomes is presented. Using a set of electrodiffusion equations, a compartmental model of a vesicle suspended in aqueous medium was studied. The light-mediated proton movement was modeled as a single proton pumping step with backpressure of the electric potential. The model fits determinations of pH obtained from PSI proteoliposomes illuminated in the presence of mediators of cyclic electron transport. The model also allows analysis of the proton gradients in relation to the transmembrane ion fluxes and electric potential. Sensitivity analysis enabled a determination of the parameters that have greater influence on steady-state levels and onset/decay rates of transmembrane pH and electric potential. This model could be used as a tool for optimizing PSI proteoliposomes for photo-electrochemical applications.

1. Introduction

The Photosystem I (PSI) reaction center is one of two multi-subunit pigment–protein complexes located in the photosynthetic membranes of cyanobacteria, algae and plants. In PSI, light induces the photo-oxidation of a specialized chlorophyll dimer, the primary electron donor known as P_{700}. After light absorption, there is a vectorial electron transfer from P_{700} to a terminal cluster, a pair of iron–sulfur molecules known as F_{A-B}, which establishes an electric potential across the complex [1]. Under normal physiological conditions most of the reducing equivalents from PSI are used for the enzymatic reduction of $NADP^+$ to NADPH. However, in the presence of an artificial redox carrier, PSI can perform a cyclic transfer of charge which is coupled to a transmembrane flux of protons [2]. A pH gradient (ΔpH) and a potential difference ($\Delta\psi$) are established, building an electrochemical potential difference for protons known as proton motive force (pmf). This photoinduced pmf is the driving force for ATP synthesis in photoshynthetic membranes, which has motivated the development of artificial systems for ATP production based on PSI reaction centers and ATP synthases co-reconstituted in liposomes [3,4]. Alternatively, other transducers of the photoinduced pmf could be inserted in the liposomal membrane, such as immobilized fluorescent dyes sensitive to ΔpH [5] or voltage-dependent ion channels [6]. The possibility of building photo-electrochemical conversion layers with these vesicles has raised the interest of using PSI for various artificial bioelectronic applications, such as those based on other photosynthetic reaction centers [7–9].

Numerous aspects of cyclic operation of PSI have been recently investigated, both on isolated photosynthetic membranes and *in vivo* [10–13]. However, the parameters controlling the extent and kinetics of ΔpH and $\Delta\psi$ when PSI is reconstituted in liposomes were not thoroughly investigated yet. These parameters are of great interest when considering the use of PSI liposomes for bio-photoelectric applications, since they will influence the operational ranges and rates. There are only a few studies that analyzed the dependence of the light-induced proton flux on parameters such as light intensity, external pH and ion concentration [4,14]. Proton movement was analyzed using the pH-sensitive fluorescent probe 9-aminoacridine (9-AA), but amplitudes and time courses of the ΔpH were discussed on a qualitative level only, as no appropriate calibration of the probe was performed.

The present study aims at a quantitative interpretation of the light-induced proton transfer across the liposomal membrane by employing a computational model. Computational models have been valuable for understanding the behavior of diverse bioenergetic systems based on lipid vesicles, as they help reduce the number of experimental procedures. Diverse proton pumps reconstituted in liposomes have been studied either by using a thermodynamic or a kinetic approach. Using irreversible thermodynamics, the kinetics of ion movements has been described for bacteriorhodopsin [15,16] and the reaction centers from

* Corresponding author. Center for Sensory–Motor Interaction (SMI), Department of Health Science and Technology, Aalborg University, Fredrik Bajers Vej 7 D3, DK-9220 Aalborg, Denmark. Tel.: +45 9940 8823; fax: +45 9815 4008.
E-mail address: cpennisi@hst.aau.dk (C.P. Pennisi).

0301-4622/$ – see front matter © 2009 Elsevier B.V. All rights reserved.
doi:10.1016/j.bpc.2009.09.013

purple bacteria [17,18]. Although quantitative expressions that fit experimental data have been obtained for these pumps, the results cannot be extrapolated to PSI because of structural and functional dissimilarities. For instance, the backpressure control exerted by the pH gradient, which limits the rate of proton translocation in these pumps [19], has not been observed in PSI preparations [4]. In addition, methods based on the thermodynamics are less attractive, since the model equations contain a number of phenomenological coefficients which are not easily available [20]. Therefore kinetic approaches are preferred, which are based on the use of electrodiffusion equations. These approaches have been mainly applied to study ATP-driven proton pumps reconstituted in liposomes. In these systems, fluorescent dyes sensitive to pH were used to follow the movement of protons and the kinetic models were determined by correlating the pH variations, ion fluxes and electric potential across the membrane of the liposomes [21–24].

In the present work, both experimental techniques and a computational model have been used to address the development of light-induced proton gradients by PSI proteoliposomes. PSI proteoliposomes were illuminated in the presence of phenazine methosulfate and ascorbate to build up a transmembrane proton gradient following cyclic transfer of charge. The magnitude of pH inside the liposomes was calculated from the fluorescence quenching of 9-AA, after an appropriate calibration that considered the effects of probe adsorption. A kinetic approach based on the electrodiffusion equations was used to build a computational model of the PSI proteoliposomes. The model fits determinations of pH under diverse experimental conditions and allows determination of the parameters that influence the rate and maximum levels of transmembrane proton gradients. In addition, the model allows analysis of the proton gradients in correlation with the transmembrane ion fluxes and electric potential.

2. Materials and methods

2.1. Materials

Chemicals of analytical grade were purchased from Sigma-Aldrich (Sigma-Aldrich Danmark A/S, Broendby, Denmark). SM-2 Bio-beads were purchased from Bio-Rad (Bio-Rad Laboratories, Copenhagen, Denmark).

2.2. Preparation of PSI proteoliposomes

PSI-200 complexes prepared from wild-type *Arabidopsis thaliana* plants were kindly provided by Prof. Poul Erik Jensen (Copenhagen University, Denmark). Complexes were suspended in Tricine buffer (20 mM Tricine–NaOH, 0.06% β-DM, pH 7.5) at a chlorophyll concentration of 0.15 mg/ml. PSI proteoliposomes were prepared according to the method described in [14], but with minor modifications. In brief, soybean phosphatidylcholine, cholesterol and phosphatidic acid (molar ratio 7:2:1) were dispersed in Tris buffer (10 mM KCl, 10 mM Tris–HCl, pH 8) to a final concentration of 10 mg/ml. The suspension was vortex-mixed and then sonicated (UP200S, Hielscher GmbH, Teltow, Germany) at an output of 30 W for 5 min, until the solution was optically clear. PS I complexes were added to the liposomes at a lipid to chlorophyll ratio of 100:1 (w/w) and then sonicated for 1 min. The sample was centrifuged at 15,000 rpm for 15 min to remove metal particles detached from the sonicator tip. To eliminate the residual detergent, the suspension was incubated with SM-2 Bio-beads (80 mg of wet beads/ml) for 1 h. The suspension containing proteoliposomes was pipetted off and stored at 4 °C.

2.3. 77 K fluorescence emission spectra

77 K fluorescence emission spectra of PS I complexes and proteoliposomes were measured with a fluorescence spectrometer (Cary Eclipse, Varian Inc., Palo Alto, CA). Chlorophylls were excited at 440 nm, and emission spectra were measured perpendicular to the exciting beam. Measurements were done at a chlorophyll concentration of 6 μg/ml for isolated PS I and 10 μg/ml for proteoliposomes.

2.4. Assay for measurement of the proton pumping activity

Proton movement across the membranes of the proteoliposomes was measured using the quenching of 9-aminoacridine (9-AA) assay [25]. Fluorescence was measured with the above mentioned fluorescence spectrometer, in which excitation was induced at 400 nm and emission was detected at 460 nm. Red actinic light was provided by a light source (Intralux 5000, Volpi AG, Schlieren, Switzerland) fitted with a red filter (low wavelength cutoff = 600 nm). The basal reaction medium consisted of Tris buffer with the addition of 0.1 μM 9-AA, 5 mM ascorbic acid and 50 μM phenazine methosulfate (PMS). The temperature of the samples was kept constant at 20 °C during the measurements.

2.5. Relating fluorescence quenching and ΔpH

The fluorescent amine 9-AA has been used as indicator of a transmembrane ΔpH in a variety of vesicular systems [4,14,25–27]. This method is based on the assumption that the neutral form of the amine is the only permeant species through the vesicle membrane and the fluorescence intensity is only proportional to the concentration in the external compartment [25]. Quenching is mainly a consequence of uptake of 9-AA into acidic vesicles, since protonated 9-AA is not fluorescent. Then, the ratio of protonated amine concentration between the inside of the vesicles and the external solution follows the proton concentration ratio. Since the amine concentration ratio can be directly related to the easily measurable fluorescence quenching, the logarithm of the quenching ratio can be used to estimate the logarithm of the proton concentration ratio (i.e. the ΔpH).

Due to adsorption of the probe to the membrane phase there is a non-linear relationship between fluorescence quenching and proton movement, which makes it difficult to obtain a quantitative measure of ΔpH [28]. However, Casadio et al. [29] developed a method to overcome that problem, given that an appropriate calibration is performed. In the present work, their calibration method was used to quantify the ΔpH in the PSI proteoliposomes preparation. PSI proteoliposomes at a chlorophyll concentration of 6 μM were allowed to equilibrate in the dark in the reaction medium used to evaluate light-triggered proton transport. Then, small volumes of 1 M NaOH were added to the sample in order to raise stepwise the external pH and the fluorescence of 9-AA was recorded as described above. In order to determine the ΔpH, the pH in the experimental cuvette was measured before and after the addition of NaOH. The ΔpH data were fitted with the empirical curve using the method of Casadio et al.:

$$\Delta pH = \frac{AQ}{(B-Q)e^{(Q/(B-Q)\ +\ CQ)}} \tag{1}$$

where Q represents the relative quenching and A, B and C are three fitting parameters. Q is defined as the ratio $(F_0-F)/F_0$, where F_0 and F are the fluorescence levels before and after addition of the NaOH aliquot ($0 \le Q \le 1$). Eq. (1) was fit using the statistical package SPSS v.15 (SPSS Inc., Chicago, IL) to obtain the values of the parameters, which resulted in $A = 14$, $B = 1.7$ and $C = -2.2$. These parameters were introduced into the Eq. (1), which was used to quantify the ΔpH from the quenching of the probe fluorescence in all the experimental procedures.

2.6. Computational model

A computational model of a single vesicle representing an average PSI proteoliposome was developed. It was assumed that the response of the whole population can be approximated with the response of

this average vesicle. The movement of charges across the membrane of the vesicle was analyzed using the two-compartment model depicted in Fig. 1, consisting in a spherical vesicle and the aqueous compartment in which it is suspended.

As mentioned before, in the presence of a redox mediator there is a cyclic electron transfer around PSI, which is illustrated in Fig. 1 using PMS as carrier. Briefly, in the presence of ascorbate, PMS becomes reduced to PMSH capturing one proton from the extravesicular compartment. PMSH is an uncharged lipophilic molecule, which penetrates the membrane and is able to efficiently donate electrons to photo-oxidized P_{700} under illumination. After two light-induced charge separations in PSI, the proton is released in the intravesicular compartment. The PMS^+ cation becomes the electron acceptor on the reducing side of PSI and the reaction cycle restarts when a new proton is captured. As shown, one reaction cycle involves two charge separations in one PSI complex and the transfer of one proton from the external solution to the intravesicular space. Consequently, it has been assumed that the vesicle contains a definite number of light-driven proton pumps in the membrane establishing a net proton flux upon illumination. This flux can be simplified to a single light-driven proton pumping step and, in a single vesicle under light-saturating conditions, it can be calculated (in mol/s) using the following formula:

$$J_{PSI} = \frac{nAkn_{H/PSI}}{N_A} \tag{2}$$

where n is the number of PSI reaction centers per unit area in the membrane, A is the area of the vesicle, k is the rate of the overall proton transfer reaction (in s^{-1}), $n_{H/PSI}$ is the number of protons transported per PSI in one entire PMS redox cycle and N_A is Avogadro's number. This flux of protons generates a transmembrane potential ($\Delta\psi$) and a proton concentration gradient (ΔpH), building the proton motive force (pmf) across the membrane:

$$pmf = \Delta\mu_{H^+} = \Delta\psi - \frac{2.3kT}{e}\Delta pH \tag{3}$$

where k is the Boltzmann constant, T is the absolute temperature and e is the electron charge. Protons and other ions present in the system can diffuse across the membrane and therefore are able to dissipate the electrochemical potential difference. The passive fluxes of protons and ions, which in the present model were restricted to K^+ and Cl^-, can be described using the Goldman–Hodgkin–Katz current equation [30]:

$$J_{ion} = P_{ion}Az_{ion}U\frac{[C_{ion}]_o - [C_{ion}]_i e^{-z_{ion}U}}{1 - e^{-z_{ion}U}} \tag{4}$$

where the sub-index *ion* represents the ionic species of interest, P is the permeability of the membrane to the ion, z is the valence of the ion, C is the concentration of the ion in the intravesicular space (i) or in the extravesicular space (o) and U is a non-dimensional potential calculated as:

$$U = \frac{\psi F}{RT} \tag{5}$$

where F is Faraday's constant and R is the universal gas constant. Whenever the potential approaches zero, the denominator in Eq. (4) was approximated with the first three terms of the series expansion of the exponential to avoid indeterminacy in the calculations.

$$J_{ion} = P_{ion}Az_{ion}\frac{[C_{ion}]_o - [C_{ion}]_i e^{-z_{ion}U}}{1 - \frac{U}{2} + \frac{U^2}{6}} \tag{6}$$

Considering the capacitive nature of the lipid bilayer, the rate of change of the electric potential across the membrane of the vesicle can be calculated from the net flux of ions J (in mol/s) using the following formula:

$$\frac{d\psi}{dt} = \frac{F}{C_m}\frac{V}{A}J \tag{7}$$

where V is the volume of the vesicle and C_m the specific capacitance of the membrane.

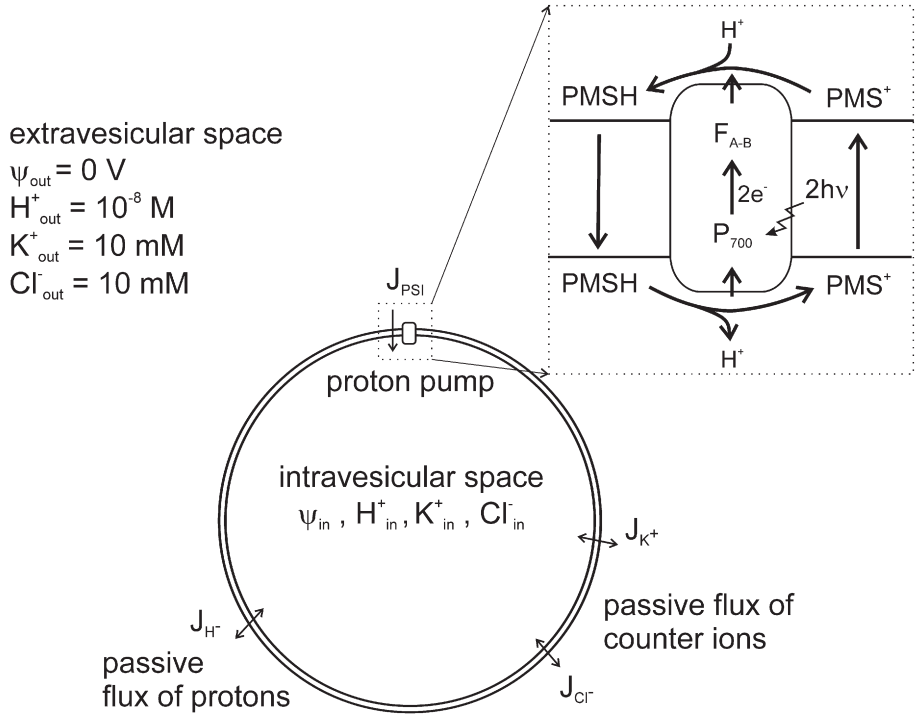

Fig. 1. Schematic representation of the implemented two-compartment model for the PSI proteoliposome, showing the main variables considered for each compartment and the fluxes between them. The scheme at the top illustrates the oxidation–reduction cycle of PMS in combination with light-induced charge separation in PSI. This reaction was considered as a single-step light-driven proton pump in the computational model.

Combining Eqs. (2) and (4) it is possible to calculate the net flux of protons which, when divided by the vesicle volume, gives the rate of change in the proton concentration inside the vesicle.

$$\frac{d[C_{H^+}]_i}{dt} = \frac{1}{V}(J_{PSI} + J_{H^+}) \tag{8}$$

Due to the internal buffering capacity (β) of the vesicles, only a small fraction of the translocated protons will be able to move freely and contribute to the pH changes. The expression that relates the internal buffer capacity with the change in the proton concentration inside the vesicle and the pH change is given by Eq. (9).

$$\beta(pH) = -\frac{d[C_{H^+}]_i}{dpH} \tag{9}$$

Finally, combining Eqs. (2), (4), (7) and (9), the two-compartment kinetic model can be described using the following set of differential equations:

$$\frac{d[C_{H^+}]_i}{dt} = \frac{1}{V}(J_{PSI} + J_{H^+})$$
$$\frac{dpH}{dt} = -\frac{1}{\beta(pH)}\frac{d[C_{H^+}]_i}{dt}$$
$$\frac{d[C_{K^+}]_i}{dt} = \frac{1}{V}J_K$$
$$\frac{d[C_{Cl^-}]_i}{dt} = \frac{1}{V}J_{Cl}$$
$$\frac{d\psi}{dt} = \frac{F}{C_m}\frac{V}{A}\left(\frac{d[C_{H^+_{total}}]_i}{dt} + \frac{d[C_{K^+}]_i}{dt} - \frac{d[C_{Cl^-}]_i}{dt}\right)$$

2.7. Solver

The previous set of differential equations, describing the rates of concentration change for all involved ions and the transmembrane potential, was implemented in Matlab v.7 (Mathworks Inc). It was solved using a predefined Matlab deterministic solver (ode23tb), appropriate for solving stiff ordinary differential equations with initial values. An ordinary differential equation problem is considered stiff if the solution being sought is varying slowly, but there are nearby solutions that vary rapidly, so the numerical method must take small steps to obtain satisfactory results. This characteristic will be noticeable as an increased number of data points for the solutions near the time when the light switches on or off.

2.8. Experimental determination of parameters of the model

2.8.1. Maximum rate of proton translocation

To estimate the maximum rate of proton translocation the initial rate approach has been used [23]. Since at the beginning of the light-induced reaction the transmembrane potential is zero, it can be assumed that the ion gradients are small and their passive movement is negligible compared with the rate of proton influx. Therefore, it is possible to estimate the maximum attainable rate of proton translocation from the initial rate of fluorescence quenching. Fluorescence quenching curves were measured in basal conditions and transformed to proton concentration changes. Using a linear interpolation function in Microsoft Excel, the first 30 s of data were interpolated and an average value for the rate was obtained.

2.8.2. Internal buffering capacity of the vesicles

The internal buffering capacity of the vesicles was determined according to the method developed by Maloney for bacterial cells [31] as modified for PSI proteoliposomes. PSI vesicles were suspended in basal Tris medium at a chlorophyll concentration of 6 μg/ml. After 15 min of equilibration in the dark, small aliquots (5 μL) of 1 N HCl were added stepwise to the sample. The changes in the external pH were measured in the range $5.5 < pH < 8$ with a pH-meter (pH 510, Oakton Instruments, Vernon Hills, IL). Both the initial (transient) and the steady-state pH values were measured, which reflected the external and the total buffering capacity, respectively. At each step, the values of external and total buffering capacities were calculated by dividing the increase in the amount of H^+ (based on the HCl added) by the increase in the pH (measured on the pH-meter). The internal buffering capacity of the vesicles at each point was obtained by simply subtracting the external from the total buffering capacity. Using an exponential interpolation function in Microsoft Excel, a function representing the average internal buffering capacity in the interval $5.5 < pH < 8$ was determined. Further details of the method are given in Appendix A.

2.8.3. Average size of the proteoliposomes

The size distribution of the proteoliposomes was determined using the dynamic light scattering instrument DynaPro 99 (Protein Solutions Inc., Charlottesville, VA). The proteoliposome sample was diluted 1:100 in Tris buffer and filtered through a 0.2 μm syringe filter. An acquisition time of 5 s was used and at least 30 acquisitions constituted a single measurement.

3. Results

3.1. Characterization of the proteoliposomes

The structural integrity of the PSI complexes after reconstitution in proteoliposomes was confirmed by measuring the fluorescence emission spectra at 77 K. Fig. 2a shows the normalized fluorescence emission spectrum at 77 K recorded from a proteoliposome sample, in comparison with the same spectrum recorded from a sample of PSI complexes suspended in buffer Tris with 0.01% β-DM. The spectrum of the control sample shows the typical peak at 730 nm, which indicates the integrity of the red wavelength emission chlorophylls in association with the complex. The spectrum of the protoliposomes also indicates chlorophyll integrity but is blue shifted by about 2 nm. There is also a small increase in the fluorescence around 670 nm, indicating the dissociation of some chlorophyll from the reaction center. The functional integrity of the electron transfer mechanism in PSI was evaluated indirectly, by measuring the transmembrane buildup of the proton gradient in response to illumination of the PSI proteoliposomes. Illumination caused a quenching of the 9-AA fluorescence, indicating a net acidification of the inner compartment of the vesicles. A typical light-induced fluorescence quenching curve measured in basal reaction medium is shown in Fig. 2a. At time $t = 30$ s the light was turned on, which produced a decrease in the fluorescence intensity as the intravesicular space started to become more acidic. After approximately 250 s of continuous illumination, the fluorescence intensity decayed to approximately 96% of its initial value. Then, the light was turned off at $t = 280$ s and the fluorescence intensity returned slowly to the initial value. The return of the fluorescence to the initial level in the dark is associated with a passive re-equilibration of the inner compartment of the vesicles with the external medium. To evaluate the nature of the light-induced pH gradients, the responses were recorded in the presence of two known ionophores. Fig. 2b shows the response to valinomycin (final concentration = 0.1 μM) and nigericin (final concentration = 7 μM). Valinomycin is an antibiotic that increases the permeability of membranes to K^+, causing a collapse of the transmembrane potential. The effect is reflected as an increased on- and off-rate of proton translocation and an increased value for the proton gradient in steady state under illumination. On the other hand, nigericin acts as a K^+/H^+ exchanger and collapses the pH gradient. The effect can be seen as a

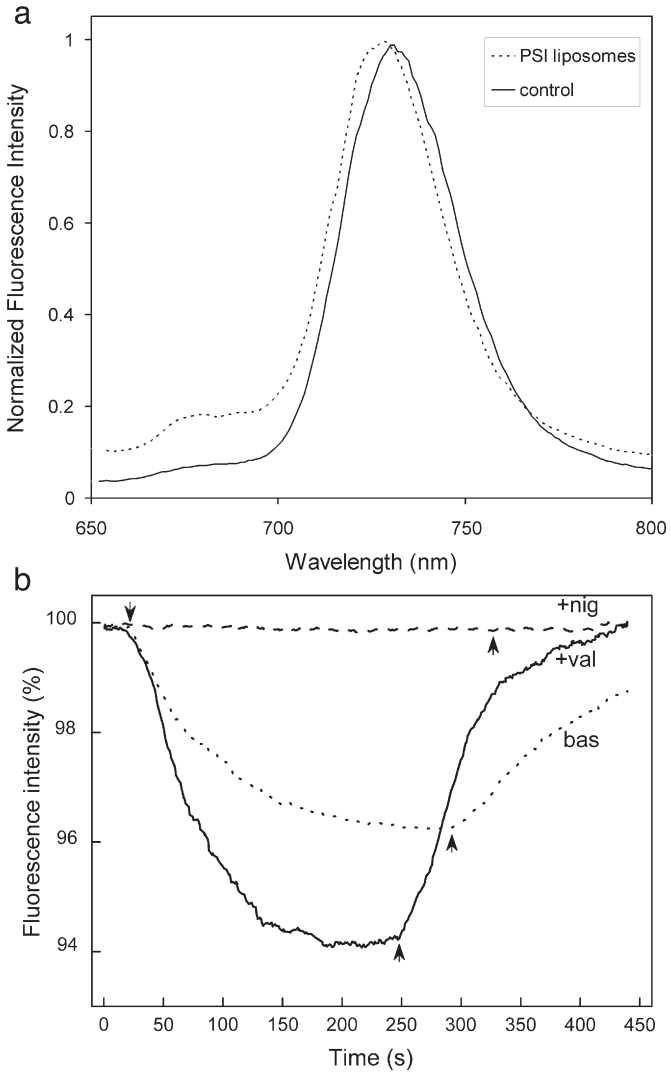

Fig. 2. Structural and functional characterization of the PSI complexes. (a) Comparison of the fluorescence emission spectra recorded at 77 K from a PSI proteoliposomes sample (dotted curve) with the one recorded from a control PSI sample (solid curve). (b) Fluorescence quenching curves indicating light-dependent proton movement in PSI proteoliposomes. The dotted curve (bas) was recorded in basal Tris medium at a chlorophyll concentration of 6 μg/ml. The solid curve (+val) is the response after addition of valinomycin to the basal medium, to a final concentration of 0.1 μM. The slashed curve (+nig) shows the response to the addition of nigericin, to a final concentration of 7 μM. Arrows indicate the time when the light was turned on (↓) and off (↑).

disappearance of the light-induced fluorescence changes, because the membrane is not able to sustain the proton gradient. The effects of both ionophores are consistent with the generation of a transmembrane potential difference caused by proton translocation.

3.2. Simulation results

Using Eq. (1), the values of ΔpH were derived from the quenching curves. These values were used to obtain the pH changes in response to illumination, which were fit with the computational model described in the methodology section. Before using the model, it was necessary to set their parameters. Some of them have been determined experimentally (e.g. average vesicle radius) and some others were extracted from the literature (e.g. specific capacitance of the membrane). A number of parameters have been adjusted until the best fit to the experimental data was obtained. The extravesicular values for all the variables (potential and concentration of protons and ions) were considered constant.

3.3. Parameters setting

3.3.1. Surface density of reaction centers, n

It was estimated from the initial lipid to chlorophyll ratio (100:1, w/w), assuming an average of 160 chlorophylls per reaction center for this preparation [32] and an average area of 0.7 nm^2 per lipid molecule [33]. The estimated value was $n = 1.5 \times 10^{10}\,cm^{-2}$. In order to adjust this parameter to the actual density of reaction centers, it was multiplied by a factor η ($\eta < 1$) that represents both the efficiency of incorporation and the number of PSI that effectively pump protons inside the vesicle upon illumination. The parameter η was adjusted during the simulations to get the best fit to the experimental curves.

3.3.2. Turnover rate, k

This parameter determines the rate at which protons are pumped across the membrane. Although there are several species participating in this process and each intermediate reaction has a unique associated rate, the overall rate will be governed by the slowest reaction and can be approximated using only one parameter [34]. Experimental evidence indicates that this parameter is affected by the transmembrane potential [4]. Therefore, an equation providing an inverse linear dependence of k on ψ was defined (Eq. (10)).

$$k(\psi) = \frac{k_{max}}{1 + \alpha\psi} \tag{10}$$

In Eq. (10), k_{max} represents the maximum attainable rate (when $\psi = 0$) and α is a parameter that establishes the degree of coupling between the transmembrane potential and the pumping rate. For a given potential value, α determines the attenuation of the rate constant: the higher the value of α the stronger the attenuation. The parameter α was initially set to $1\,V^{-1}$, implying an attenuation of 17% to the rate constant when the transmembrane potential reaches 200 mV. Its value was adjusted during the simulations to give the best fit to the experimental data. After using the approach described in the Materials and methods section, the average value obtained for k_{max} was $28 \pm 2\ s^{-1}$ ($n = 5$).

3.3.3. Number of protons transported per PSI in a complete redox cycle, $n_{H/PSI}$

This parameter was set to 1, according to what was previously described in Fig. 1 in relation to the cycle of translocation of protons mediated by PSI in vesicles when PMS is the soluble carrier [35,36]. Under light-saturation conditions the charge separation reactions within PSI are far faster than those associated with the diffusion of species across the membrane. Therefore it is reasonable to assume that only one reaction center is providing the two electrons required for translocation of 1 proton.

3.3.4. Membrane permeabilities, P_{ion}

For the equations involving the flux of protons and the other ions, the membrane permeabilities were set initially to values obtained from the literature (see Table 1). These values were then adjusted to obtain the best fit to the experimental data.

3.3.5. Buffering capacity, β

The internal buffering capacity was determined in the range of $5.5 < pH < 8$ on three independent samples (Fig. A1, Appendix A). Although the buffering capacity is usually considered constant over a given pH range, it has been observed that a variable buffering capacity gives a better fit to the data in models of vesicle acidification [24]. Thus, the data shown in Fig. A1 were interpolated with an exponential function to obtain an expression relating the buffering capacity with the pH in the range of interest. The expression is given in Eq. (11).

$$\beta(pH) = 1.15 \times 10^{-5} e^{1.042pH} \tag{11}$$

Table 1
Permeabilities of the ions involved in the model, in cm/s.

Permeability	Symbol	Initial value	Reference	Final value
Proton	P_H^+	1.5×10^{-3}	[52]	2×10^{-4}
Potassium	P_K^+	1.7×10^{-12}	[51]	1×10^{-12}
Chloride	P_{Cl}^-	7.6×10^{-11}	[63]	7×10^{-12}

The initial values were extracted from the literature, while the final values were those used in the simulation of the average vesicle in basal medium.

3.3.6. Specific capacitance of the membrane

The specific capacitance of the membrane was set to 1 μF/cm^2, the standard estimate value used for phospholipids bilayers.

3.3.7. Radius of the average vesicle

The radius of the average vesicle was obtained by averaging the distributions of the hydrodynamic radius of the proteoliposomes from three independent samples. The histogram from the preparations used in this work followed a log-normal distribution (data not shown), which is expected for vesicles prepared with sonication [37]. The estimated radius of the average vesicle was 42 ± 2 nm.

3.4. Fitting the basal responses of PSI proteoliposomes

Fig. 3 shows experimental results corresponding to the light-induced pH changes recorded in a sample containing PSI liposomes in basal reaction medium. The curve was fit by simulating a vesicle with a diameter of 42 nm. The ion permeabilities and the parameters η and α were adjusted until the RMS error between the experimental and the simulation curves was minimized. Ion permeabilities were finally adjusted to the values indicated in Table 1, while the other parameters resulted in $\eta=0.3$ and $\alpha=40$.

3.5. Fitting the responses of PSI proteoliposomes to valinomycin

The ionophore valinomycin has the known property of being a passive potassium transporter across lipid membranes. Therefore, the effect of an increased concentration of valinomycin was simulated by simply increasing the potassium permeability. However, as shown in Fig. 4, several values of increased potassium permeability did not adjust the model to the measured response to valinomycin. By further investigation, it was found that valinomycin could also affect the proton permeability [38,39]. Then, by introducing an increase in the proton permeability of the vesicles it was possible to fit the output of the model to the experimental curves. The best fit was obtained for a potassium permeability increase of 1000 times accompanied by a proton permeability of 1.1×10^{-2} cm/s (an increase of approximately 55 times from its initial value). Fig. 5 shows the adjustment of the model to the experimental curve using the assumption of the combined effect.

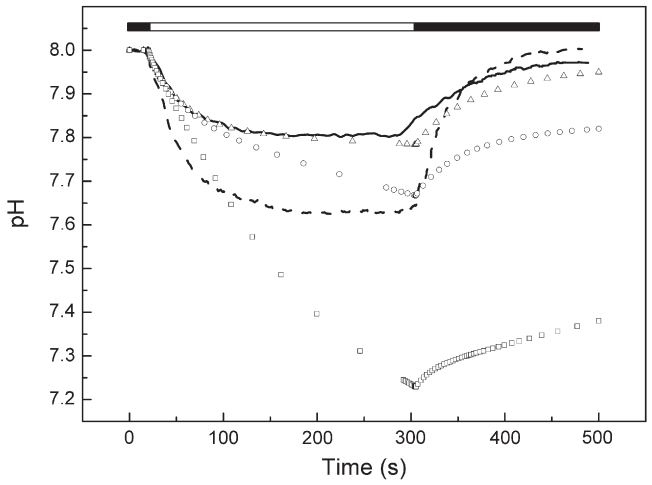

Fig. 4. Failure to predict the effect of valinomycin by an increase of the potassium permeability alone. The solid curve is the light-induced response from Fig. 3 and the slashed curve is the response after addition of valinomycin to a final concentration of 0.1 μM. The dots are the estimations of the model, which were obtained increasing the permeability to potassium 10 (triangles), 100 (circles) and 1000 times (squares).

3.6. Estimation of the concentration of ions and the membrane potential

The solution to the model equations, apart from the pH curves shown in Figs. 3–5, contains the light- and time-dependent values for the intravesicular concentration of K^+ and Cl^- ions and for the membrane potential. These values were obtained for the two situations described in the preceding paragraphs, i.e. the basal response and the response to valinomycin, and are presented in Fig. 6. In order to evaluate the time- and light-dependent effect of the

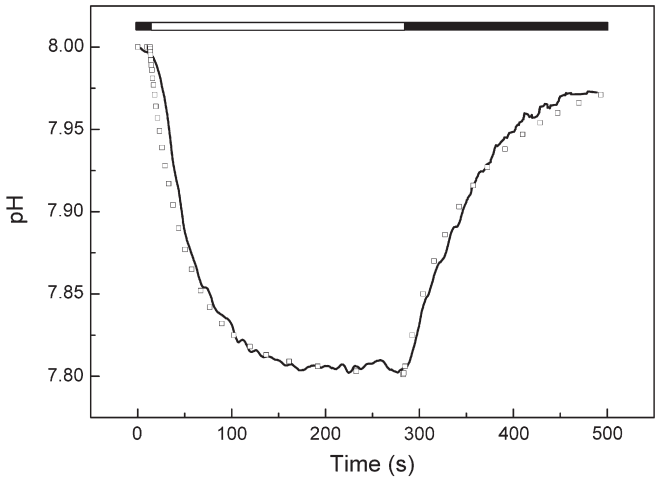

Fig. 3. Light-induced responses of PSI proteoliposomes in basal conditions. The solid curve was calculated from fluorescence quenching data obtained from PSI proteoliposomes in Tris medium at a chlorophyll concentration of 6 μg/ml. The square dots were calculated using the model. The white area in the bar at the top represents the period of illumination.

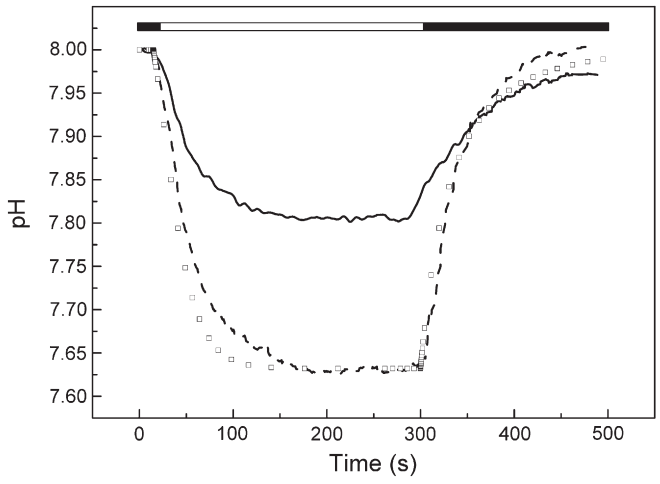

Fig. 5. The effect of valinomycin is predicted by a simultaneous increase of the permeabilities for potassium and protons. As in Fig. 4, the light-induced responses in basal medium (solid curve) and after addition of valinomycin (slashed curve) are shown. The square dots are estimations of the model, obtained by increasing the potassium permeability 1000 times and the proton permeability to 1.1×10^{-2} cm/s.

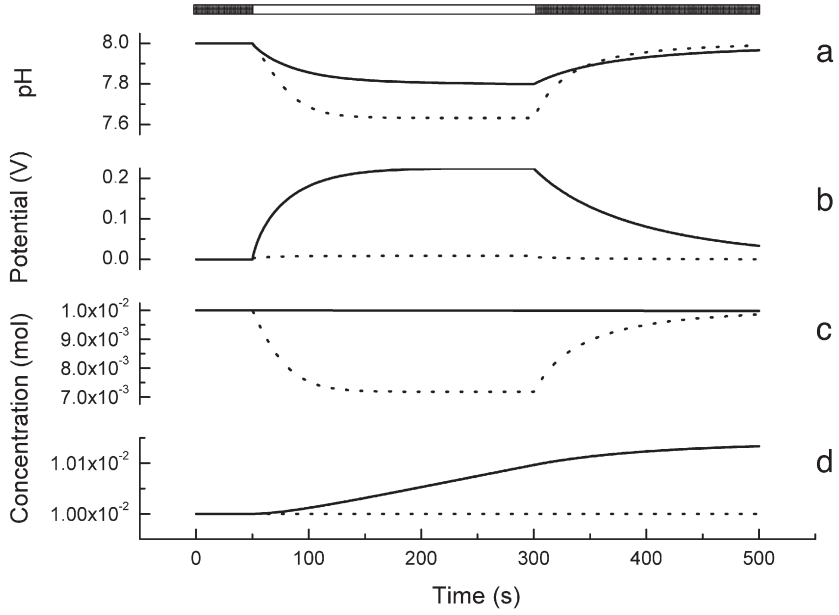

Fig. 6. Outputs of the model. The curves represent the estimations of the pH (a), membrane potential (b), concentration of potassium and (c) concentration of chloride (d). The results were obtained after simulation of basal conditions (solid curves) and addition of valinomycin (dotted curves).

ion fluxes on the membrane potential, the first derivatives for the intravesicular concentrations of H^+, K^+ and Cl^- were also calculated. They are plotted in Fig. 7 together with the transmembrane potential, giving an indication of the direction of the transmembrane ion fluxes in response to illumination and during passive equilibration in the dark. The model was evaluated in basal conditions (Fig. 7a and b) and considering the presence of valinomycin (Fig. 7c and d).

3.7. Sensitivity analysis

Sensitivity analysis was performed to identify which of the model parameters have higher impact on the magnitude and rates of the transmembrane pH and electric potential. The initial values of the model parameters were those used to fit the responses of the vesicles in basal medium. The most relevant parameters were selected and their initial values were changed by $\pm 10\%$. The results obtained after performing simulations with the modified parameters are summarized in Table 2. The model outputs that were evaluated include the steady-state values of pH and potential differences (ΔpH_{ss} and $\Delta\psi_{ss}$) and the values of the half-time after light is switched on (τpH_{on} and $\tau\psi_{on}$) or off (τpH_{off} and $\tau\psi_{off}$).

3.8. Simulation of an increased transmembrane proton gradient

Some of the model parameters were adjusted with the aim of comparing the output of the model with data previously obtained from PSI preparations. Using PSI complexes having an average of 90 chlorophylls per P_{700} and detergent mediated reconstitution, Cladera et al. prepared PSI proteoliposomes with an average radius of 60 nm [4]. In the presence of 0.1 μM valinomycin, the average steady-state pH differences were 1.8 ± 0.3 pH units. Although the time constants were not reported, they can be estimated from a figure showing the light-induced pH changes (Fig. 4 in Ref. [4]). The estimations are a half-time for acidification of 45 s and a half-time for passive re-equilibration of 153 s. Using the model that fit the responses of our vesicles in valinomycin, the radius of the average vesicle was increased to 60 nm. Then, the product ($n \times \eta$) was increased to 2 to reflect the increased density of reaction centers and the more efficient incorporation reported in Cladera et al. Under these conditions, the magnitude of the steady-state pH difference was 0.8 pH units, the half-time for acidification was 8 s and the half-time for passive re-equilibration was 18 s. But the preparation of Cladera et al. showed slower kinetics and a bigger steady-state pH difference, therefore an additional modification was introduced to the model. To simulate tighter vesicles, the ion permeabilities were decreased one order of magnitude. This resulted in a steady-state pH difference of 1.2 pH units, a half-time for acidification of 28 s and a half-time for passive re-equilibration of 159 s. The results are shown in Fig. 8. Since the two counter ions (protons and potassium) have quite different kinetics of charge transfer in this situation, it can be noticed that the membrane potential displays a transient overshoot. This reflects the effects of both an increased proton influx rate and a decreased potassium efflux rate.

4. Discussion

4.1. Characterization of the PSI preparation

PSI proteoliposomes were prepared by means of sonication, a methodology which is normally used to produce vesicles containing functional PSI complexes [14,40,41]. Sonication is generally chosen due to its inherent simplicity, but the mechanical energy delivered during sonication may cause disruption of membrane proteins [42]. In addition, the procedure may also induce the presence of aggregates (e.g. non-incorporated complexes and/or non-vesicular accumulations of lipids). Therefore, the PSI proteoliposomes used in this work were analyzed to determine the integrity of PSI and the presence of aggregates.

The fluorescence emission spectrum at 77 K of the PSI proteoliposomes was consistent with the spectral properties of the complexes in suspension (Fig. 2), which indicated structural integrity of PSI after incorporation. The blue shift is indicative of modification of the microenvironment around the chlorophyll molecules after reconstitution, which does not imply a major structural change [43]. However, there was an increase in the amount of free chlorophyll indicating that a minor fraction (~10%) of the pigment–protein complexes was disrupted. In addition, the functional integrity of the electron transfer chain was demonstrated by the ability of the

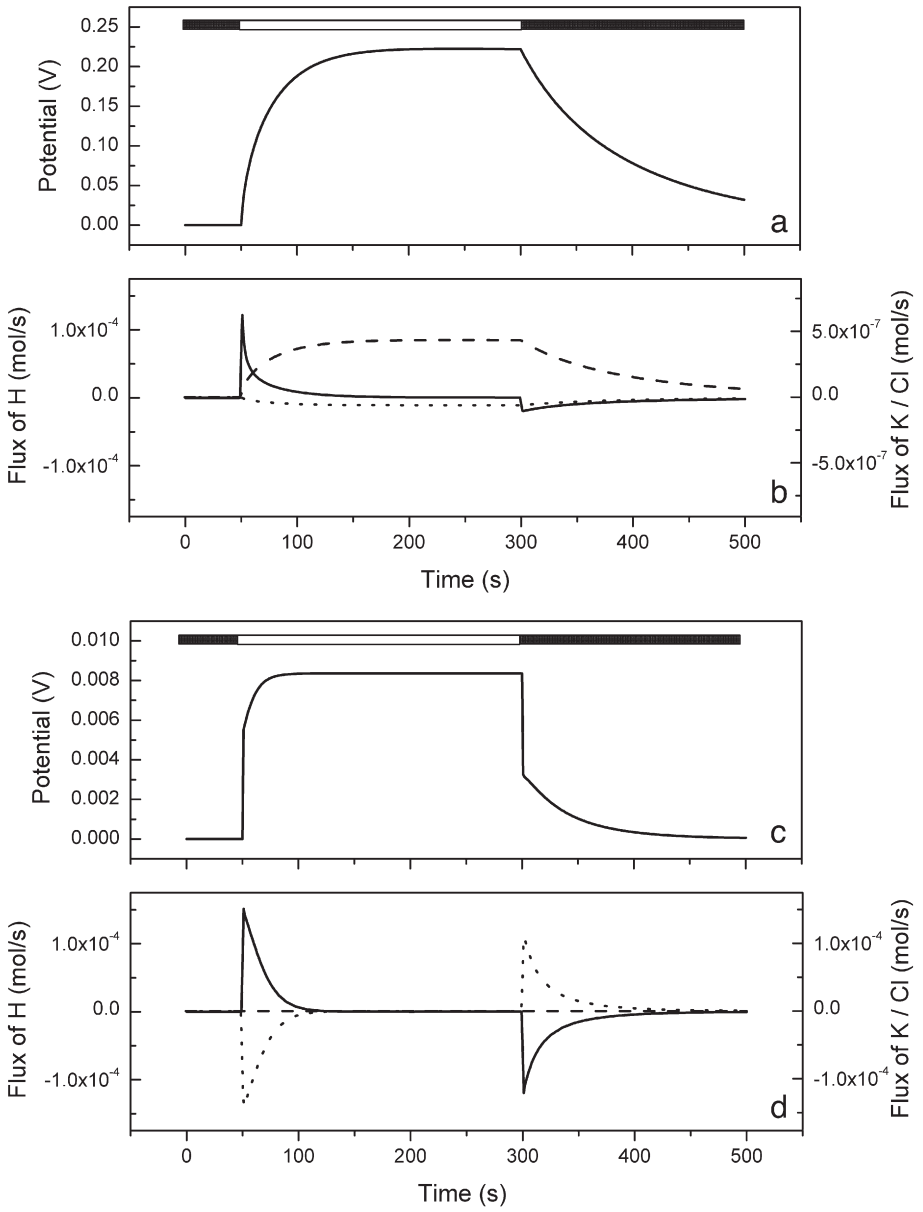

Fig. 7. Correlation of the potential with the light-induced ionic fluxes. The curves (a) and (c) are the estimations of the transmembrane potential obtained with the model, in basal conditions and in the presence of valinomycin, respectively. The curves (b) and (d) are the first derivatives of the intravesicular ion concentrations, showing the flux of protons (solid curve), potassium (dotted curve) and chloride ions (dashed curve). Notice the change in scale for the K^+ and Cl^- fluxes in (b).

proteoliposomes to sustain light-induced transmembrane proton movement mediated by extrinsic carriers (ascorbate and PMS). The intravesicular pH of the PSI proteoliposomes decreased in response to illumination, concurring with those reported in the literature using similar PSI preparations [4,14]. Finally, the histograms obtained after measurement of the radii of the vesicles showed no

Table 2
Sensitivity analysis of the ΔpH, $\Delta\psi$ and their corresponding onset and decay half-times.

Parameter	Variable					
	ΔpH_{ss}	τpH_{on}	τpH_{off}	$\Delta\psi_{ss}$	$\tau\psi_{on}$	$\tau\psi_{off}$
Surface density of PSI	5/−5	−3/3	0/0	4/−4	−3/3	0/0
Buffering capacity	−10/9	3/−4	3/−3	2/−2	4/−4	4/−4
Turnover rate k_{max}	5/−5	−3/3	0/0	4/−4	−3/3	0/0
α	−4/10	1/7	2/4	−3/4	1/−1	2/−7
Vesicle radius	−9/10	3/−5	2/−4	2/−2	4/−4	4/−4
H^+ permeability	−4/5	−6/7	−8/9	−4/4	−6/7	−8/9
K^+ permeability	0.1/−0.1	0.2/−0.2	0.2/−0.4	<±0.1	<±0.1	<±0.1
Cl^- permeability	1/−1	2/−2	1/−1	−0.2/0.2	−0.3/0.3	−1/1

The parameters of the model were varied ±10% and the resulting percent changes in the output variables are given. Percentages corresponding to 10% increments are given at the left side of the slash, while those corresponding to 10% decrements are given at the right side.

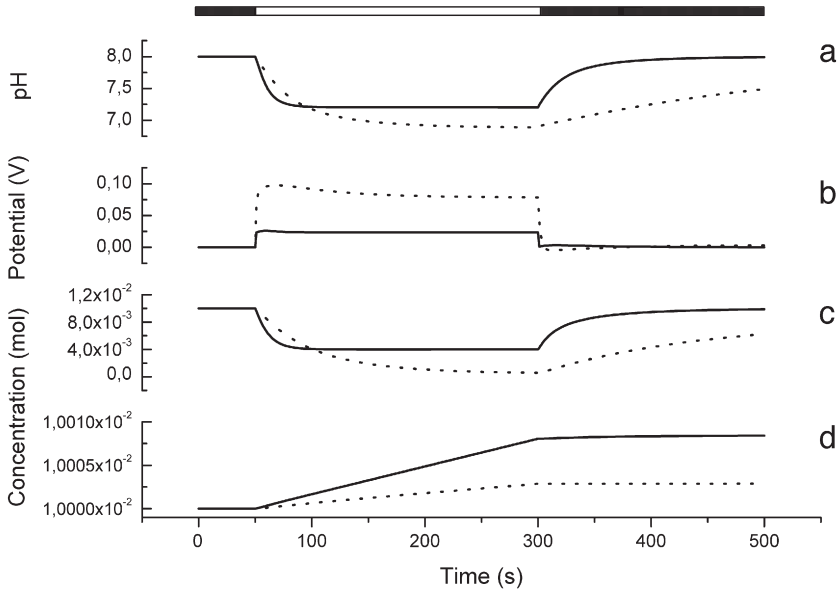

Fig. 8. Simulation of an increased pH gradient. The curves represent the estimates of the pH (a), membrane potential (b), concentration of potassium and (c) concentration of chloride (d). The results were obtained after simulation of vesicles in valinomycin, using a radius of 60 nm for the average vesicle and an increased density of reaction centers (solid curves). In addition to these modifications, the permeabilities for all ions were decreased one order of magnitude (dotted curves).

secondary peaks, indicating the absence of aggregates (data not shown).

4.2. Model for the PSI proteoliposomes

The light-induced transmembrane proton movement is the result of a series of complex chemical reactions that involve photo-induced charge separation in PSI and transmembrane movement of charged species. However, a simplified analysis of the problem was possible thanks to the use of a computational model. Specifically, the active proton transfer step, which involves cyclic charge transfer by the PSI reaction centers and redox cofactors, was modeled as a proton pump with a single time constant that was only affected by the backpressure of the membrane potential. Although light intensity and ionic strength are known to affect the rate of electron transfer in PSI vesicles [4,44,45], these parameters were kept constant to reduce the complexity of the model. An additional factor that affects the efficiency of proton translocation is the concentration of the redox carrier PMS. While maximal rates of charge transfer have been observed in the range of 20 μM to 70 μM PMS, concentrations outside this range appear to inhibit the redox cycle [3,4,46]. The experiments in the present work were therefore performed at constant PMS concentration (50 μM) and in consequence the model does not incorporate PMS concentration as a variable.

A model involving cyclic electron transfer across PSI was previously developed by Cruz et al. to describe the contribution of $\Delta\psi$ to the steady-state pmf in thylakoids [47]. In their model, they have also assumed that proton transport due to cyclic electron transfer could be modeled with a single step proton pump. However, this pump was affected by the backpressure of the ΔpH, since a decrease in the pH restricted electron flow at the cytochrome b_6f complex. The authors neglected the backpressure of $\Delta\psi$ on the rate of proton pumping, as they assumed it was considerably smaller than the backpressure of ΔpH. In contrast, in our preparations the only transmembrane complex involved in the cyclic electron transport is PSI. Consequently, there is no backpressure of the ΔpH while the backpressure of $\Delta\psi$ becomes substantial. This aspect of our model confirms what was already stated by Cladera et al., who suggested that the backpressure effect of the ΔpH can be discarded for PSI proteoliposomes [4].

To model the transmembrane movement of charged species a set of electrodiffusion equations were defined. The passive movement of ions was based on the Fick's diffusion law combined with the Goldman–Hodgkin–Katz current equation for electrodiffusive flux. Similarly, this approach predicted with high degree of accuracy the magnitudes of the ionic fluxes in vesicles in which the proton gradients were generated by ATP-driven proton pumps [21–24]. Finally, the membrane potential was obtained considering the bilayer as a capacitor and its value was obtained from the variation of the net current across the membrane with time.

4.3. Simulation results

There was a high degree of adjustment between the experimental values and the output of the model, except during the beginning of the light-induced reaction and the end of the dark phase after illumination (Figs. 3 and 4). The deviations of the model at the beginning and at the end of the experimental curves might be related to the fact that there is a distribution rather than a single value for the permeabilities. This might influence the active and passive kinetics, taking into consideration that it has been assumed that an average vesicle would represent the average behavior of a population having a relatively wide distribution of sizes. As it has been previously shown, that approximation is better for narrow distributions, when the vesicle population approaches the permeability kinetics of a homogeneous population [48]. Regarding the final values for the membrane permeability to ions (Table 1), differences up to one order of magnitude in comparison to the literature were observed. This is not surprising, since the membrane permeability is specific to the liposomal preparation used. Among other factors, it may depend upon vesicle size, presence of incorporated proteins, presence of traces of detergent, surface charge and lipid purity. For instance, there have been reported values ranging from 10^{-9} to 10^{-4} for the proton permeability [38,49–52].

It has been often been assumed that valinomycin only affects the membrane permeability to potassium, since the very high affinity of potassium ions to this ionophore [53] causes a significant increase of the potassium flux through lipid membranes [54–56]. Micromolar concentrations of valinomycin can increase 2 to 4 orders of magnitude the membrane conductance to potassium [55,57,58]. According to

this, the initial attempt was to simulate the effect of valinomycin by increasing 10 to 1000 times the permeability to potassium (Fig. 4). It was found that the model could not predict the effect of this ionophore by an increase of the potassium permeability alone. As shown in Fig. 5, the effect could only be explained by a simultaneous increase of permeabilities to potassium and protons. When the permeability to potassium was increased three orders of magnitude (1000 times), it was found that there was good agreement between the simulations and the experimental data after the proton permeability was increased to 1.1×10^{-2} cm/s. This finding is consistent with previous reports, where it was found that valinomycin is responsible of a small fraction of proton transport across the membrane of liposomes [38,39]. It was suggested that proton permeability could be facilitated by the formation of short-lived complexes of valinomycin–potassium with anionic forms of free fatty acids [59]. More recently, valinomycin was shown to form a stable complex with protons in the form of H_3O^+ ions, indicating that valinomycin could serve as a carrier for proton transfer across biological membranes [60].

After fitting the pH curves, the fluxes for the counter ions and the membrane potential were simultaneously estimated by the model (Fig. 7). With respect to the fluxes for the counter ions, it can be seen that in basal conditions they follow the movement of protons but in opposite directions and with slower kinetics. Potassium tends to escape from the vesicles and chloride tends to enter, as it can be seen in Fig. 7b. The relative magnitude of the fluxes when compared with that for protons is related with the relative values for the membrane permeabilities. In basal conditions the increase of the membrane potential is mostly due to the increase of the positive charge inside the vesicles (Fig. 7a). Only when valinomycin is present, the flux of potassium becomes comparable to that of protons, almost canceling the membrane potential (Fig. 7c and d). The steady-state value of membrane potential was about 200 mV, which is comparable to the 200 to 300 mV membrane potential of proton gradients that drive ATP synthesis in the thylakoids [2]. In addition, the value is also comparable to the 180 mV value measured in proteoliposomes prepared with reaction centers from purple bacteria [17]. In this case, it is reasonable to assume that the potential difference is smaller due to the backpressure of the ΔpH on the light-induced proton transport. With respect to the time course of the transmembrane potential, the predictions of our model are consistent with qualitative measurements of light-induced electric potential performed by Barsky et al., in which the light-induced potential of PSI proteoliposomes followed also exponential patterns of onset and decay [61].

4.4. Sensitivity analysis

The steady-state value of ΔpH depends mostly upon buffering capacity and size of the vesicles, while the on and off time constants are more sensitive to proton permeability (Table 2). Increased values of buffering capacity or larger vesicles make it more difficult for the establishment of a transmembrane proton gradient. On the other hand, the steady-state value of $\Delta\psi$ is mostly dependent on the density of PSI complexes and the turnover rate. Proton permeability affects both the time constants and the steady-state values of $\Delta\psi$.

The sensitivity data presented in Table 2 could be helpful when considering the use of PSI proteoliposomes as photo-electrochemical converters. Depending whether the energy is primarily detected in the form of a membrane potential or a pH gradient, different strategies of optimization could be applied. For instance, large values of steady-state potential could be obtained by using large vesicles with a high density of reaction centers. On the other hand, large pH differences with a fast onset rate could be obtained by using small sized vesicles and reducing the backpressure of the potential including valinomycin on the reaction medium. It's important that the rates at which the events occur in the described system could be too slow for some applications while acceptable for some others. The kinetics of ion movement reported here is faster than that reported for proteoliposomes prepared with reaction centers of purple bacteria used in photoelectric converters [62]. This is due to the fact that PMS is an efficient mediator of cyclic electron transfer of charges, while soluble quinones used as exogenous carriers for purple bacteria reaction centers have a slow diffusional movement. For other applications, such as the proposed use of PSI for fast depolarization of voltage-gated ion channels, the response time reported here is unacceptable, unless a more efficient mechanism to transfer the mobile charges is found.

4.5. Simulation of an increased transmembrane proton gradient

Although the magnitude of the pH gradients obtained in this work was about 1/9 of the value previously reported for PSI proteoliposomes, the time course of the light-induced fluorescence quenching curves reported here are quite consistent with those reported previously [4]. When the validity of the model was tested in conditions where an increased pH gradient is produced, it was shown that an increased ΔpH could be obtained by increasing the value of $(n\times\eta)$ in the model (Fig. 8). This indicates that the smaller proton gradient reported here could be due to the uncontrolled orientation of the PSIs and lower incorporation efficiency. The increase in the value of $(n\times\eta)$ caused a decrease in the half-times for onset and passive re-equilibration, which was re-adjusted by reducing the membrane permeabilities of the ions. These results are consistent with the fact that it is not possible to control protein orientation in the membrane of proteoliposomes prepared by sonication, while PSI proteoliposomes prepared by detergent mediated reconstitution have good asymmetric protein orientation and low permeability values [42]. In addition, vesicles with ion-tight membranes have also reduced vesicle permeability to both PMS and ascorbate, which increases the efficiency of the light-induced proton transfer [4]. However, this situation could not be tested as these parameters have not been introduced in the model. Overall, these results suggest that the model could potentially be used to fit measurements obtained from other PSI preparations.

4.6. Conclusion

The light-induced protonmotive force buildup in PSI proteoliposomes is the result of a series of reactions involving photo-induced charge separation in PSI, charge transfer to soluble redox mediators and transmembrane movement of ions and carriers. Although the microscopic detail of these reactions is complex, we have shown in this work that it is possible to quite accurately describe the magnitude and kinetics of ΔpH and $\Delta\psi$ using a simple computational approach. It has been shown that a model based on a set of electrodiffusion equations combined with a proton pump with backpressure for $\Delta\psi$, makes it possible not only to fit quite accurately light-induced pH changes but also to predict the changes in ion concentrations and transmembrane potential of the vesicles. In addition, the results of this work support the capability of valinomycin to increase proton permeability across biological membranes. This model provides a useful tool to analyze light-induced protonmotive force buildup in PSI proteoliposomes, which might also be used as a platform for other models describing transmembrane ion gradients and membrane potential across membranes supporting electrogenic pumps. This model also represents a potential new tool to determine the most efficient combination of parameters in applications intended to use PSI proteoliposomes as photo-electrochemical converters.

Acknowledgments

We are grateful to Poul Erik Jensen (Copenhagen University, Denmark) for providing the PSI complexes and for his advice in relation to the experimental procedures. We also wish to thank to

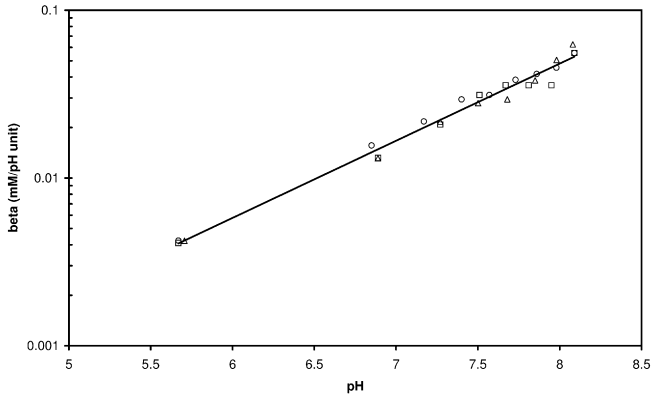

Fig. A1. The internal buffer capacity β in terms of the pH. The data points represent three independent measurements, which are identified by different symbols (circles, squares or triangles). The correlation coefficient of the exponential fit was 0.96.

Daniel Otzen (Aarhus University, Denmark) for facilitating the dynamic light scattering equipment and the fluorescence spectrometer and to Miguel Rodriguez Jr. (Oak Ridge National Laboratory, USA) for providing PSI preparations used in preliminary experiments.

This work was supported by the Danish Research Agency and the Sygekassernes Helsefond, Denmark and the Office of Biological and Environmental Research, U.S. Department of Energy. Oak Ridge National Laboratory is managed by UT-Battelle, LLC for the U. S. Department of Energy under Contract No. DE-AC05-00OR22725.

Appendix A. Experimental determination of the buffer capacity function β(pH)

According to the method of Maloney [31], the internal buffering capacity of the vesicles can be obtained by substracting the external from the total buffering capacity:

$$\beta_{\text{int}} = \beta_{\text{tot}} - \beta_{\text{ext}} = \frac{\Delta H^+}{\Delta pH_{ss}} - \frac{\Delta H^+}{\Delta pH_t} \quad \text{(A1)}$$

where ΔH^+ is the change in the amount of protons caused by addition of HCl, and ΔpH_{ss} and ΔpH_t are corresponding steady state and transient pH changes. After applying the procedure to three independent samples, the values of internal buffering capacity computed using equation A1 are shown in Fig. A1.

References

[1] W. Leibl, B. Toupance, J. Breton, Photoelectric characterization of forward electron transfer to iron–sulfur centers in photosystem I, Biochemistry 34 (1995) 10237–10244.
[2] B. Ke, Proton translocation and ATP synthesis, in: B. Ke (Ed.), Photosynthesis — Photobiochemistry and Photobiophysics, Kluwer, Dodrecht, 2001.
[3] G. Hauska, D. Samoray, G. Orlich, N. Nelson, Reconstitution of photosynthetic energy-conservation. 2. Photophosphorylation in liposomes containing photosystem-I reaction center and chloroplast coupling-factor complex, Eur. J. Biochem. 111 (1980) 535–543.
[4] J. Cladera, J.L. Rigaud, H. Bottin, M. Dunach, Functional reconstitution of photosystem I reaction center from cyanobacterium Synechocystis sp PCC6803 into liposomes using a new reconstitution procedure, J. Bioenerg. Biomembranes 28 (1996) 503–515.
[5] T. Nguyen, K.P. McNamara, Z. Rosenzweig, Optochemical sensing by immobilizing fluorophore-encapsulating liposomes in sol–gel thin films, Anal. Chim. Acta 400 (1999) 45–54.
[6] E. Greenbaum, M. Humayun, T. Kuritz, J.W. Lee, C.A. Sanders, B. Bruce, J. Millsaps, I. Lee, Application of photosynthesis to artificial sight, Proc. Annu. Int. Conf. IEEE Eng. Med. Biol. Soc. 4 (2001) 4089–4091.
[7] S. Ajiki, H. Sugino, H. Toyotama, M. Hara, J. Miyake, Reconstitution and immobilization of photo-reaction units from photosynthetic bacterium *Rhodopseudomonas viridis*, Mater. Sci. Eng. C 6 (1998) 285–290.
[8] K.B. Lam, E.A. Johnson, M. Chiao, L. Lin, A MEMS photosynthetic electrochemical cell powered by subcellular plant photosystems, J. Microelectromech. Syst. 15 (2006) 1243–1250.
[9] Y. Lu, J. Xu, B. Liu, J. Kong, Photosynthetic reaction center functionalized nanocomposite films: effective strategies for probing and exploiting the photo-induced electron transfer of photosensitive membrane protein, Biosens. Bioelectron. 22 (2007) 1173–1185.
[10] Y. Munekage, M. Hashimoto, C. Miyake, K. Tomizawa, T. Endo, M. Tasaka, T. Shikanai, Cyclic electron flow around photosystem I is essential for photosynthesis, Nature 429 (2004) 579–582.
[11] T.J. Avenson, A. Kanazawa, J.A. Cruz, K. Takizawa, W.E. Ettinger, D.M. Kramer, Integrating the proton circuit into photosynthesis: progress and challenges, Plant Cell Environ. 28 (2005) 97–109.
[12] P. Joliot, A. Joliot, Quantification of cyclic and linear flows in plants, Proc. Natl. Acad. Sci. U. S. A. 102 (2005) 4913–4918.
[13] T. Shikanai, Cyclic electron transport around photosystem I: genetic approaches, Annu. Rev. Plant Biol. 58 (2007) 199–217.
[14] G. Orlich, G. Hauska, Reconstitution of photosynthetic energy-conservation. 1. Proton movements in liposomes containing reaction center of photosystem-I from spinach-chloroplasts, Eur. J. Biochem. 111 (1980) 525–533.
[15] H.V. Westerhoff, B.J. Scholte, K.J. Hellingwerf, Bacteriorhodopsin in liposomes. I. A description using irreversible thermodynamics, Biochim. Biophys. Acta 547 (1979) 544–560.
[16] K.J. Hellingwerf, J.C. Arents, B.J. Scholte, H.V. Westerhoff, Bacteriorhodopsin in liposomes. II. Experimental evidence in support of a theoretical model, Biochim. Biophys. Acta 547 (1979) 561–582.
[17] D. Molenaar, W. Crielaard, K.J. Hellingwerf, Characterization of protonmotive force generation in liposomes reconstituted from phosphatidylethanolamine, reaction centers with light-harvesting complexes isolated from *Rhodopseudomonas palustris*, Biochemistry 27 (1988) 2014–2023.
[18] B.J. van Rotterdam, W. Crielaard, I.H.M. van Stokkum, K.J. Hellingwerf, H.V. Westerhoff, Simplicity in complexity: the photosynthetic reaction center performs as a simple 0.2 V battery, FEBS Lett. 510 (2002) 105–107.
[19] B.J. van Rotterdam, H.V. Westerhoff, R.W. Visschers, D.A. Bloch, K.J. Hellingwerf, M.R. Jones, W. Crielaard, Pumping capacity of bacterial reaction centers and backpressure regulation of energy transduction, Eur. J. Biochem. 268 (2001) 958–970.
[20] S. Schuster, R. Ouhabi, M. Rigoulet, J. Mazat, Modelling the interrelation between the transmembrane potential and pH difference across membranes with electrogenic proton transport upon build-up of the proton-motive force, Bioelectrochem. Bioenerget. 45 (1998) 181–192.
[21] A.B. Bennett, R.M. Spanswick, Optical measurements of deltapH and deltaV in corn root membrane vesicles: kinetic analysis of Cl^- effects on a proton-translocating ATPase, J. Membr. Biol. 71 (1983) 95–107.
[22] D. Brauer, S. Tu, A. Hsu, C.E. Thomas, Kinetic analysis of proton transport by the vanadate-sensitive ATPase from maize root microsomes, Plant Physiol. 89 (1989) 464–471.
[23] D.P. Briskin, I. Reynolds-Niesman, Determination of H^+/ATP stoichiometry for the plasma membrane H^+-ATPase from red beet (*Beta vulgaris* L.) storage tissue, Plant Physiol. 95 (1991) 242–250.
[24] M. Grabe, G. Oster, Regulation of organelle acidity, J. Gen. Physiol. 117 (2001) 329–343.
[25] S. Schuldiner, H. Rottenberg, M. Avron, Determination of pH in chloroplasts. 2. Fluorescent amines as a probe for the determination of pH in chloroplasts, Eur. J. Biochem. 25 (1972) 64–70.
[26] R. Casadio, B.A. Melandri, The behavior of 9-aminoacridine as an indicator of transmembrane pH difference in liposomes of natural bacterial phospholipids, J. Bioenerg. Biomembranes 9 (1977) 17–29.
[27] Y. Evron, R.E. McCarty, Simultaneous measurement of ΔpH and electron transport in chloroplast thylakoids by 9-aminoacridine fluorescence, Plant Physiol. 124 (2000) 407–414.
[28] S. Grzesiek, N.A. Dencher, The 'delta pH'-probe 9-aminoacridine: response time, binding behaviour and dimerization at the membrane, Biochim. Biophys. Acta 938 (1988) 411–424.
[29] R. Casadio, S. Di Bernardo, P. Fariselli, B.A. Melandri, Characterization of 9-aminoacridine interaction with chromatophore membranes and modelling of the probe response to artificially induced transmembrane ΔpH values, Biochim. Biophys. Acta, Biomembr. 1237 (1995) 23–30.
[30] B. Hille, Ion Channels of Excitable Membranes, Sinauer Associates Inc, Sunderland, USA, 2001.
[31] P.C. Maloney, Membrane H^+ conductance of *Streptococcus lactis*, J. Bacteriol. 140 (1979) 197–205.
[32] J.A. Ihalainen, P.E. Jensen, A. Haldrup, I.H.M. Van Stokkum, R. Van Grondelle, H.V. Scheller, J.P. Dekker, Pigment organization and energy transfer dynamics in isolated photosystem I (PSI) complexes from *Arabidopsis thaliana* depleted of the PSI-G, PSI-K, PSI-L, or PSI-N subunit, Biophys. J. 83 (2002) 2190–2201.
[33] B.A. Lewis, D.M. Engelman, Lipid bilayer thickness varies linearly with acyl chain length in fluid phosphatidylcholine vesicles, J. Mol. Biol. 166 (1983) 211–217.
[34] M. Schonfeld, M. Montal, G. Feher, Functional reconstitution of photosynthetic reaction centers in planar lipid bilayers, Proc. Natl. Acad. Sci. U. S. A. 76 (1979) 6351–6355.
[35] M. Miller, L.C. Petersen, F.B. Hansen, P. Nicholls, Effect of ionophores on carrier-mediated electron translocation in ferricyanide-containing liposomes, Biochem. J. 184 (1979) 125–131.
[36] R.C. Prince, S.J.G. Linkletter, P.L. Dutton, The thermodynamic properties of some commonly used oxidation–reduction mediators, inhibitors and dyes, as determined by polarography, Biochim. Biophys. Acta, Bioenerg. 635 (1981) 132–148.

[37] B.G. Tenchov, T.K. Yanev, M.G. Tihova, R.D. Koynova, A probability concept about size distributions of sonicated lipid vesicles, Biochim. Biophys. Acta, Biomembr. 816 (1985) 122–130.
[38] J.W. Nichols, D.W. Deamer, Net proton-hydroxyl permeability of large unilamellar liposomes measured by an acid–base titration technique, Proc. Natl. Acad. Sci. U. S. A. 77 (1980) 2038–2042.
[39] P.S. Brookes, D.F.S. Rolfe, M.D. Brand, The proton permeability of liposomes made from mitochondrial inner membrane phospholipids: comparison with isolated mitochondria, J. Membr. Biol. 155 (1997) 167–174.
[40] K. Sigfridsson, O. Hansson, P. Brzezinski, Electrogenic light reactions in photosystem. 1. Resolution of electron-transfer rates between the iron–sulfur centers, Proc. Natl. Acad. Sci. U. S. A. 92 (1995) 3458–3462.
[41] Z. Yang, X. Su, F. Wu, Y. Gong, T. Kuang, Photochemical activities of plant photosystem I particles reconstituted into phosphatidylglycerol liposomes, J. Photochem. Photobiol., B Biol. 78 (2005) 125–134.
[42] J.L. Rigaud, B. Pitard, D. Levy, Reconstitution of membrane proteins into liposomes: application to energy-transducing membrane proteins, Biochim. Biophys. Acta Bioenerg. 1231 (1995) 223–246.
[43] Z. Yang, X. Su, F. Wu, Y. Gong, T. Kuang, Effect of phosphatidylglycerol on molecular organization of photosystem I, Biophys. Chem. 115 (2005) 19–27.
[44] H. Ishikawa, M. Hirano, T. Takabe, Reconstitution of highly purified P700-chlorophyll-a protein complexes into galactosyldiacylglycerol liposomes, Agric. Biol. Chem. 48 (1984) 3011–3018.
[45] S. Hoshina, S. Itoh, Characterization of photosystem I chlorophyll–protein complexes reconstituted into phosphatidylcholine liposomes, Plant Cell Physiol. 28 (1987) 599–609.
[46] A.T. Jagendorf, M. Avron, Cofactors and rates of photosynthetic phosphorylation by spinach chloroplasts, J. Biol. Chem. 231 (1958) 277–290.
[47] J.A. Cruz, C.A. Sacksteder, A. Kanazawa, D.M. Kramer, Contribution of electric field ($\Delta\psi$) to steady-state transthylakoid proton motive force (pmf) in vitro and in vivo. Control of pmf parsing into $\Delta\psi$ and ΔpH by ionic strength, Biochemistry 40 (2001) 1226–1237.
[48] S. Clerc, Y. Barenholz, A quantitative model for using acridine orange as a transmembrane pH gradient probe, Anal. Biochem. 259 (1998) 104–111.
[49] N.R. Clement, J. Michael Gould, Pyranine (8-hydroxy-1, 3, 6-pyrenetrisulfonate) as a probe of internal aqueous hydrogen ion concentration in phospholipid vesicles, Biochemistry 20 (1981) 1534–1538.
[50] Y. Nozaki, C. Tanford, Proton and hydroxide ion permeability of phospholipid vesicles, Proc. Natl. Acad. Sci. U. S. A. 78 (1981) 4324–4328.
[51] S. Paula, A.G. Volkov, A.N. Van Hoek, T.H. Haines, D.W. Deamer, Permeation of protons, potassium ions, and small polar molecules through phospholipid bilayers as a function of membrane thickness, Biophys. J. 70 (1996) 339–348.
[52] R.H. Gensure, M.L. Zeidel, W.G. Hill, Lipid raft components cholesterol and sphingomyelin increase H^+/OH^- permeability of phosphatidylcholine membranes, Biochem. J. 398 (2006) 485–495.
[53] Y.A. Ovchinnikov, Ionophores and channels, Int. J. Quant. Chem. 20 (1981) 461–478.
[54] T.E. Andreoli, M. Tieffenberg, D.C. Tosteson, The effect of valinomycin on the ionic permeability of thin lipid membranes, J. Gen. Physiol. 50 (1967) 2527–2545.
[55] G. Stark, R. Benz, The transport of potassium through lipid bilayer membranes by the neutral carriers valinomycin and monactin — experimental studies to a previously proposed model, J. Membr. Biol. 5 (1971) 133–153.
[56] R. Benz, G. Stark, K. Janko, P. Lauger, Valinomycin mediated ion transport through neutral lipid membranes: influence of hydrocarbon chain length and temperature, J. Membr. Biol. 14 (1973) 339–364.
[57] H. Ginsburg, G. Stark, Facilitated transport of di and trinitrophenolate ions across lipid membranes by valinomycin and nonactin, Biochim. Biophys. Acta 455 (1976) 685–700.
[58] H. Ginsburg, M.T. Tosteson, D.C. Tosteson, Some effects of trinitrocresolate and valinomycin on Na and K transport across thin lipid bilayer membranes: a steady-state analysis with simultaneous tracer and electrical measurements, J. Membr. Biol. 42 (1978) 153–168.
[59] A. Fogt, Complexes of valinomycin–K^+ and FFAs as proton carriers across lipid membranes, Cell. Mol. Biol. Lett. 7 (2002) 182.
[60] J. Kriz, J. Dybal, E. Makrlik, Valinomycin–proton interaction low-polarity media, Biopolymers 82 (2006) 536–548.
[61] E.L. Barsky, Z. Dancshazy, L.A. Drachey, M.D. Il'ina, A.A. Jasaitis, A.A. Kondrashin, V. D. Samuilov, V.P. Skulachev, Reconstitution of biological molecular generators of electric current. Bacteriochlorophyll and plant chlorophyll complexes, J. Biol. Chem. 251 (1976) 7066–7071.
[62] E.Y. Katz, A.Y. Shkuropatov, O.I. Vagabova, V.A. Shuvalov, Coupling of photoinduced charge separation in reaction centers of photosynthetic bacteria with electron-transfer to a chemically modified electrode, Biochim. Biophys. Acta 976 (1989) 121–128.
[63] L.T. Mimms, G. Zampighi, Y. Nozaki, C. Tanford, J.A. Reynolds, Phospholipid vesicle formation and transmembrane protein incorporation using octyl glucoside, Biochemistry 20 (1981) 833–840.